Crystal size induced reduction in thermal hysteresis of Ni-Ti-Nb shape memory thin films

Cite as: Appl. Phys. Lett. **108**, 171907 (2016); https://doi.org/10.1063/1.4948377
Submitted: 18 February 2016 . Accepted: 16 April 2016 . Published Online: 29 April 2016

K. Li, Y. Li, K. Y. Yu, C. Liu, D. Gibson, A. Leyland, A. Matthews, and Y. Q. Fu

Crystal size induced reduction in thermal hysteresis of Ni-Ti-Nb shape memory thin films

K. Li,[1,2,3] Y. Li,[1,2,a)] K. Y. Yu,[4] C. Liu,[5] D. Gibson,[6] A. Leyland,[5] A. Matthews,[5] and Y. Q. Fu[3,a)]

[1]*School of Materials Science and Engineering, Beihang University, Beijing 100191, China*
[2]*Beijing Key Laboratory for Advanced Functional Materials and Thin Film Technology, Beihang University, Beijing 100191, China*
[3]*Department of Physics and Electrical Engineering, Faculty of Engineering and Environment, Northumbria University, Newcastle Upon Tyne NE1 8ST, United Kingdom*
[4]*Department of Materials Science and Engineering, China University of Petroleum, Beijing 102249, China*
[5]*School of Materials, University of Manchester, ICAM, Pariser Bldg., Manchester M1 7JR, United Kingdom*
[6]*Institute of Thin Films, Sensors and Imaging, University of the West of Scotland, Scottish Universities Physics Alliance, Paisley PA1 2BE, United Kingdom*

(Received 18 February 2016; accepted 16 April 2016; published online 29 April 2016)

$Ni_{41.7}Ti_{38.8}Nb_{19.5}$ shape memory alloy films were sputter-deposited onto silicon substrates and annealed at various temperatures. A narrow thermal hysteresis was obtained in the Ni-Ti-Nb films with a grain size of less than 50 nm. The small grain size, which means an increase in the volume fraction of grain boundaries, facilitates the phase transformation and reduces the hysteresis. The corresponding less transformation friction and lower heat transfer during the shear process, as well as reduced spontaneous lattice distortion, are responsible for this reduction of the thermal hysteresis. *Published by AIP Publishing*. [http://dx.doi.org/10.1063/1.4948377]

In aerospace and biomedical fields, selecting the optimum materials for applications of micropumps and microvalves in micro-electromechanical systems (MEMS), miniature systems, and energy storage devices has been a key issue in the past few decades.[1–6] NiTi-based shape memory films have been considered as one of the most promising candidates due to their high power output per volume, large actuation strain, and high damping capacity.[7] For many micro-actuators, a narrow hysteresis is essential to improve the efficiency of actuation, whereas for energy storage devices a wide hysteresis is required. Therefore, much attention has been paid to developing NiTi-based films with a tailorable thermal hysteresis.[8,9] So far two alloying methods have been suggested to be effective: (1) adding a third or fourth soluble element, such as Cu and Pd, into the NiTi film to obtain improved geometric compatibility between martensite and austenite;[10–12] and (2) adding a third element with a limited solubility, such as Ag and W, into NiTi matrix and modulating thermal hysteresis through grain refinement or internal stress around NiTi grains to change the paths of phase transformation.[13,14] Besides alloying, annealing has been considered as a subsequent tool to tune the hysteresis of alloyed NiTi by changing the grain size, as demonstrated in Ni-Ti-Nb bulk alloys, in which their thermal hysteresis is tuned through changing the grain size by adjusting the annealing temperature.[15] However, the grain size dependence of hysteresis in the Ni-Ti-Nb thin films is barely investigated to date. The phase transformation and physical properties of Ni-Ti-Nb thin films might be different from their bulk counterparts for several reasons.[1] First, the crystallization paths are distinct as the sputtered thin films are crystallized from a non-equilibrium amorphous state on a single crystal substrate whereas the bulk alloys solidify through a near-equilibrium process. This might lead to different textures and grain boundary structures of the materials. Second, residual stress and 2D geometry of thin films may supply additional constraints to the nucleation and growth of the martensite, in contrast to bulk alloys where those effects are less significant. The present work is thus focused on manipulating the phase transformation behavior and hysteresis of Ni-Ti-Nb shape memory films by post-deposition annealing, and grain size dependent phase transformation is discussed.

Ni-Ti-Nb films were deposited onto four inch Si (100) wafers at room temperature using a DC magnetron sputtering system with a $Ni_{50}Ti_{50}$ (at. %) target and a pure Nb target. The substrates were attached to a holder which was rotated at a speed of ~60 cycles per minute. Base pressure of the chamber was 2×10^{-3} Pa and the work pressure was 0.6 Pa. After deposition, the films were sealed into quartz tubes under high vacuum ($<10^{-5}$ Pa) and annealed at 550 °C, 575 °C, 600 °C, 625 °C, and 650 °C for 30 min, respectively. For all the samples, the heating rate was kept at 5 °C per minute and natural cooling in the furnace was adapted. The films were 2 μm in thickness, and the composition was identified as $Ni_{41.7}Ti_{38.8}Nb_{19.5}$, measured using electron probe microanalysis (EPMA, JXA-8100). Microstructures were acquired from X-ray diffraction (XRD, SmartLab with a Cu-Kα radiation ($\lambda = 0.15409$ nm)) and cross-sectional transmission electron microscopy (TEM, JEM-2100F). The phase transformation behavior was assessed using the four probe electrical resistivity method, by cooling the sample from room temperature down to −270 °C using liquid helium.

Fig. 1(a) shows the XRD patterns of both the as-deposited and annealed Ni-Ti-Nb films. The pattern of the as-deposited sample shows wide peaks with low intensities, which indicates

a)Authors to whom correspondence should be addressed. Electronic addresses: liyan@buaa.edu.cn and Richard.fu@northumbria.ac.uk

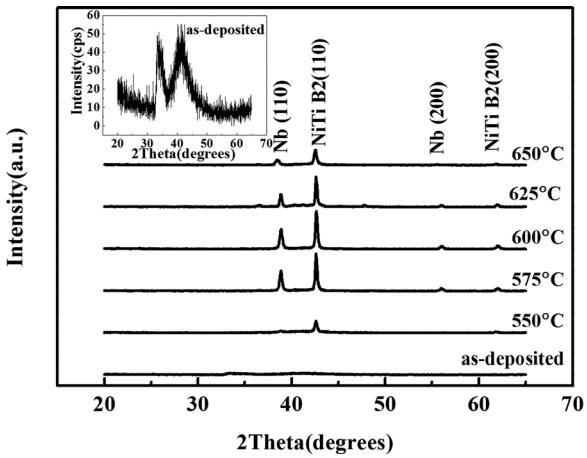

FIG. 1. XRD results of as-deposited and annealed Ni-Ti-Nb thin films; the inset is the enlarged curve of the as-deposited sample.

extremely small nano-grains embedded inside an amorphous matrix as shown in the inset. The appearance of nano-grains may be attributed to the increase of the substrate temperature (up to 100 °C) during the sputtering process. The sample annealed at 550 °C is partially crystallized, whereas a fully crystalline NiTi(Nb) matrix with Nb-rich grains is obtained when the samples were annealed at or above 575 °C, as demonstrated by the XRD profile. Compared with Ref. 16, all the peaks that represent Nb-rich grains are found to shift toward higher angles. This may be attributed to the solution effects, where the Nb atoms were replaced by the Ti atoms, thus resulting in a decrease in the lattice spacing of Nb-rich grains.[17]

Fig. 2 shows the TEM images and the corresponding diffraction patterns of the as-deposited sample and the samples annealed at 600 °C and 625 °C. The as-deposited sample exhibits an amorphous dominant state as shown in Fig. 2(a).

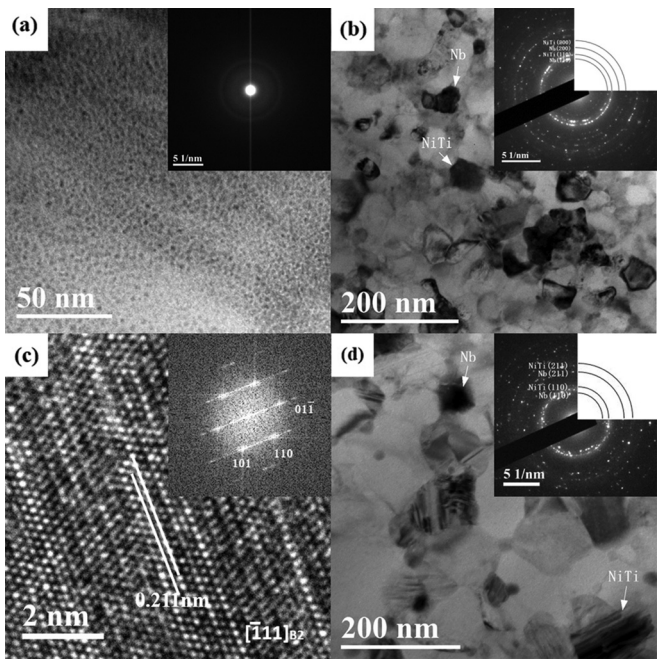

FIG. 2. TEM images of (a) as-deposited sample, (b) sample annealed at 600 °C, and (d) sample annealed at 625 °C. Insets are the corresponding SAED patterns. (c) The [1̄11] axis HRTEM image of the sample annealed at 600 °C and its corresponding FFT pattern.

The mixed crystalline structures of both NiTi(Nb) and Nb-rich grains can be identified from Figs. 2(b) and 2(d). Fig. 2(c) is the [1̄11] axis high resolution transmission electron microscopy (HRTEM) pattern of a representative grain in the sample annealed at 600 °C and its corresponding Fast Fourier Transformation (FFT) pattern. NiTi(Nb) and Nb-rich crystals were identified using scanning transmission electron microscopy (STEM), and the average grain size of NiTi(Nb) grains was calculated from the data of more than 20 NiTi(Nb) grains for each sample. The estimated average grain sizes of NiTi(Nb) phase are 48 nm and 78 nm for the samples annealed at 600 °C and 625 °C, respectively. The lamellar structures in both images were identified as Moiré fringes, which could be attributed to the overlapping of nano-grains.

Fig. 3 shows the electrical resistance vs temperature (ER-T) curves of the Ni-Ti-Nb film samples. For the as-deposited sample and the sample annealed at 550 °C, a negative temperature coefficient of resistivity (TCR) was obtained, i.e., the electrical resistivity decreases with increasing temperature. This phenomenon has been observed in many non-magnetic amorphous metals.[18] As the amorphous phase is dominant in these two samples, the mean free path of conducting electrons in the amorphous phase could be dominated by the weak localization effects and enhanced interaction between electrons.[18] The two small "pop-outs" in the curve of 550 °C-annealed sample might be attributed to the relatively large internal stress in the composite of amorphous matrix and nano-size grains. The different extents of contraction between the amorphous matrix and the nano-size grains during cooling

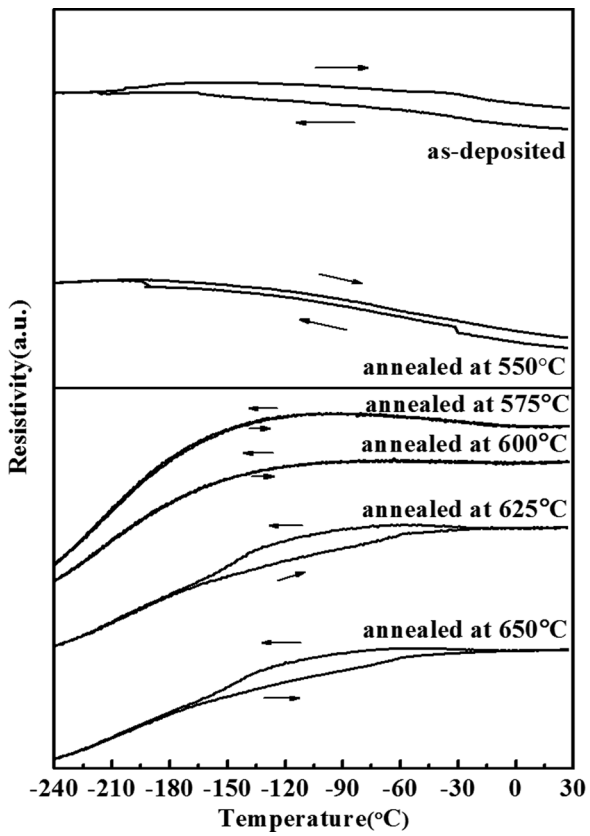

FIG. 3. Electrical resistance-temperature (ER-T) curves of the as-deposited Ni-Ti-Nb thin film and those annealed at 550 °C, 575 °C, 600 °C, 625 °C, and 650 °C, respectively.

result in internal stress, which may lead to local deformation and enhance the scattering. Thus the resistivity is shifted.[19]

For the samples annealed at 575 °C and 600 °C, a positive value of TCR was obtained, i.e., the electrical resistivity increases with increasing temperature. For both the samples, the profiles of resistivity as a function of temperature show a similar trend, i.e., the cooling and heating curves almost overlap each other. The phase transformations can be identified from the increases of resistance during heating and decreases of resistance during cooling, which gradually occur over a wide temperature range till a low temperature. This also indicates the existence of a near-zero thermal hysteresis in the martensitic transformation that occurred in the samples annealed at intermediate temperatures.

The ER-T profiles of the film annealed at higher temperatures of 625 °C and 650 °C in Fig. 3 show well-defined hysteresis in the heating and cooling curves, which is commonly observed in the bulk NiTiNb shape memory alloys, indicating the generation of a well-defined martensitic phase transformation.[17]

In order to demonstrate the shape memory effect, a piece of peeled off free-standing film that was annealed at 600 °C has been pre-deformed in liquid nitrogen. The deformed film maintained its shape in liquid nitrogen after removing the applied force. When taken out of liquid nitrogen and warmed up in air, the film returned to its original shape immediately. The shape recovery demonstration has been repeated at least three times without any degradation.

Clearly, there are significant differences in the hysteresis between the films annealed at 600 °C and 625 °C. This can be attributed to the changes in the grain size obtained at different annealing temperatures. Possible reasons are listed below.

First, the thermal hysteresis in the ER-T curves of the shape memory alloy is mainly due to the differences in energy dissipation and release of latent heat during phase transformation upon heating/cooling. It is well known that phase transformations originate from the local reconstructions of a few atoms.[20] When the grain size becomes small enough, large amount of grain boundaries will promote the phase transformation since there are more defects, and the phase transformation is more easily to occur there.[20] This would facilitate the martensitic transformation and the reverse transformation, resulting in a narrow thermal hysteresis, as indicated in the overlapped ER-T curves shown in Fig. 3.[21,22] Second, the thermal hysteresis in the martensitic transformation originates from the friction energy in the interfacial movement during the shear process. Decreasing grain sizes will shorten the movement distance and reduce the energy dissipation.[23] Finally, as the grain size of the NiTi(Nb) domains decreases, the spontaneous lattice distortion is reduced,[24] which means that a lower energy barrier between the parent phase and the martensite phase is formed and thus facilitates the phase transformation.[25]

In summary, the thermal hysteresis of the $Ni_{41.7}Ti_{38.8}Nb_{19.5}$ thin films is found to be highly dependent on the grain size, which can be controlled through the annealing process. The decrease in the grain size of NiTi(Nb) phase results in an increased volume fraction of grain boundaries, which favors the transformation due to their defect nature. The reduction in grain size also reduces the energy dissipation in transformation friction and weakens the lattice distortions, which reduces the energy barriers and facilitates the process of phase transformation. Thus, tuning the thermal hysteresis via controlling the grain size is applicable in the $Ni_{41.7}Ti_{38.8}Nb_{19.5}$ thin films.

This work is supported by the National Basic Research Program of China (No. 2012CB619400) and the National Natural Science Foundation of China (NSFC, No.51171009). Funding supports from the UoA and CAPEX funding from Northumbria University at Newcastle upon Tyne and Royal Academy of Engineering: Research Exchange between UK and China are acknowledged. K.Y. acknowledges financial support from CUPB (2462015YQ0602).

[1]Y. Q. Fu, H. J. Du, W. M. Huang, S. Zhang, and M. Hu, Sens. Actuators, A **112**, 395 (2004).
[2]W. Ni, Y. T. Cheng, and D. S. Grummon, Appl. Phys. Lett. **80**, 3310 (2002).
[3]G. A. Shaw, D. D. Stone, A. D. Johnson, A. B. Ellis, and W. C. Crone, Appl. Phys. Lett. **83**, 257 (2003).
[4]X. G. Ma and K. Komvopoulos, Appl. Phys. Lett. **83**, 3773 (2003).
[5]T. Zhao, Y. Li, Y. Xiang, X. Zhao, and T. Zhang, Surf. Coat. Technol. **205**, 4404 (2011).
[6]T. Zhao, Y. Li, Y. Liu, and X. Zhao, J. Mech. Behav. Biomed. Mater. **13**, 174 (2012).
[7]S. Miyazaki and A. Ishida, Mater. Sci. Eng., A **273–275**, 106 (1999).
[8]C. Chluba, W. W. Ge, R. L. Miranda, J. Strobel, L. Kienle, E. Quandt, and M. Wuttig, Science **348**, 1004 (2015).
[9]D. Dye, Nat. Mater. **14**, 760 (2015).
[10]J. Cui, Y. S. Shu, O. O. Famodu, Y. Furuya, J. Hattrick-Simpers, R. D. James, A. Ludwig, S. Thienhaus, M. Wuttig, Z. Zhang, and I. Takeuchi, Nat. Mater. **5**, 286 (2006).
[11]R. Zarnetta, R. Takahashi, M. L. Young, A. Savan, Y. Furuya, S. Thienhaus, B. Maaβ, M. Rahim, J. Frenzel, H. Brunken, Y. S. Chu, V. Srivastava, R. D. James, I. Takeuchi, G. Eggeler, and A. Ludwig, Adv. Funct. Mater. **20**, 1917 (2010).
[12]X. L. Meng, H. Li, W. Cai, S. J. Hao, and L. S. Cui, Scr. Mater. **103**, 30 (2015).
[13]P. S. Buenconsejo, R. Zarnetta, D. König, A. Savan, S. Thienhaus, and A. Ludwig, Adv. Funct. Mater. **21**, 113 (2011).
[14]C. Zamponi, M. Wuttig, and E. Quandt, Scr. Mater. **56**, 1075 (2007).
[15]M. Piao, S. Miyazaki, and K. Otsuka, Mater. Trans., JIM **33**, 346 (1992).
[16]J. Li, H. F. Wang, J. Liu, and J. M. Ruan, Mater. Sci. Eng., A **609**, 235 (2014).
[17]M. Wang, M. Jiang, G. Liao, S. Guo, and X. Zhao, Prog. Nat. Sci.: Mater. Int. **22**, 130 (2012).
[18]U. Mizutani, Phys. Status Solidi B **176**, 9 (1993).
[19]U. Chandni, A. Ghosh, H. S. Vijaya, and S. Mohan, Appl. Phys. Lett. **92**, 112110 (2008).
[20]A. Talis and V. Kraposhin, Acta Cryst. A **70**, 616 (2014).
[21]A. Ahadi and Q. P. Sun, Appl. Phys. Lett. **103**, 021902 (2013).
[22]A. Ahadi and Q. P. Sun, Acta Mater. **90**, 272 (2015).
[23]Y. Kim, G. Cho, S. Hur, S. Jeong, and T. Nam, Mater. Sci. Eng., A **438–440**, 531 (2006).
[24]H. X. Zong, Z. Ni, X. D. Ding, T. Lookman, and J. Sun, Acta Mater. **103**, 407 (2016).
[25]Q. S. Sun, A. Ahadi, M. P. Li, and M. X. Chen, Sci. China: Technol. Sci. **57**, 671 (2014).